

Figure 2. (a) Top: ORTEP diagram of the central core structure of Y_2Cu_4 . (b) Bottom: Diagram showing the arrangement of metal atoms in the central core.

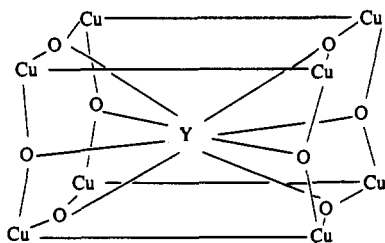
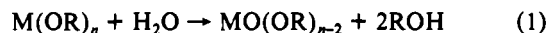


Figure 3. Diagram showing the bonding environment of Y and Cu atoms in the 1-2-3 superconductor.

$Cu_4OCl_6L_4$ ($L = OPEt_3, Py, NH_3$) molecules.^{5d} This dicopper unit is perpendicular to the other dicopper unit.

The most important feature in this molecule is the central core unit of Y_2Cu_4 . In this unit, there are two oxide ligands, each of which bridges two yttrium atoms and two copper atoms. The $Y(1)-Y(1')$ separation is 3.785 (8) Å. The separations of yttrium atoms bridged by oxygen atoms in previous reported homonuclear yttrium compounds span a considerable range, 3.3–4.0 Å.^{6,11} The yttrium atoms are also bridged to the copper atoms through the oxygen atoms on the PyO^- ligands. In addition, a nitrate ligand is coordinated to the yttrium atom. As a result, the yttrium atom is surrounded by eight oxygen atoms. If the nitrate coordinated to the yttrium atom was replaced by another unit of Cu_4O_2 , the

environment of the yttrium and the copper atoms in the central core of this molecule would remarkably resemble that found in the oxygen-deficient perovskite structure⁷ of the $YBa_2Cu_3O_{7-x}$ superconductor as shown in Figures 2 and 3. As found in the structure of the 1-2-3 superconductor, the four copper atoms and the two oxide ligands are approximately in the same plane with the maximum deviation (± 0.010 (5) Å) of $Cu(3)$ and $Cu(3')$ from the plane. The $Cu(3)-O(7)-Cu(4)$ angle, 109 (1)°, is, however, much smaller than that in $YBa_2Cu_3O_{7-x}$ (about 165°), apparently caused by the additional chloride ligand. The four oxygen atoms $O(2)$, $O(3)$, $O(5)$, and $O(6)$ are approximately in the same plane with the $Y(1)$ atom and coordinate to $Y(1)$ in a square-planar fashion: $O(2)-Y(1)-O(3) = 178.0$ (8)°; $O(5)-Y(1)-O(6) = 174.1$ (8)°. Within the Y_2Cu_4 unit the $Y-Cu$ separations are $Y(1)-Cu(3) = 3.422$ (6) Å, $Y(1)-Cu(3') = 3.392$ (7) Å, $Y(1)-Cu(4) = 3.353$ (6) Å, and $Y(1)-Cu(4') = 3.334$ (7) Å. The distance $Cu(3)-Cu(4')$ is very long, 4.74 Å. Therefore, the geometry of this Y_2Cu_4 unit could be best described as two tetrahedra sharing the common edge $Y(1)-Y(1')$ (Figure 2b). Although there are a few recent reports describing bimetallic Ln-Cu compounds in which the Ln and Cu atoms are bridged either by a hydroxy ligand^{8a} or a PyO^- ligand,^{8b} to our knowledge, bimetallic Ln-Cu or Y-Cu compounds with oxide bridges are previously unknown. In fact, the Y_2Cu_8 compound described here is the first example of bimetallic Y-Cu compounds. The formation of oxide ligands in this molecule is not unexpected. There have been several reports describing the formation of oxide ligands in the yttrium-alkoxide system.⁹ It has been suggested¹⁰ by Caulton and Hubert-Pfalzgraf that a hydrolysis process (eq 1) might account for the formation of the O^{2-} ligand.



Although the major product **2** has not been fully characterized, it appears to have the composition¹¹ of $Y_2Cu_8(PyO)_4(O)_2(NO_3)_4(H_2O)_4$, based on the result of elemental analysis. Both compounds **1** and **2** dissolve readily in water and yield green solutions, which undergo rapid hydrolysis and produce a light blue powder, presumably a mixture of metal oxides and hydroxides. The further characterization of compound **2** and the hydrolysis process is underway. The syntheses of bimetallic complexes with different ratios of yttrium and copper atoms and trimetallic compounds containing barium, yttrium (lanthanides), and copper atoms are in progress. Efforts have also been taken to study the magnetic interactions of multiple paramagnetic copper(II) centers in this system.

Acknowledgment. I thank the University of Windsor for supporting this research.

Supplementary Material Available: Details of the X-ray diffraction analysis, listings of atomic coordinates, crystallographic data, thermal parameters, bond lengths, and bond angles, and an ORTEP diagram for the entire molecule (16 pages); a table of calculated and observed structure factors (14 pages). Ordering information is given on any current masthead page.

Department of Chemistry and Biochemistry
University of Windsor
Windsor, Ontario, N9B 3P4 Canada

Suning Wang

Received December 4, 1990

- (6) (a) Poncelet, O.; Hubert-Pfalzgraf, L. G. *Inorg. Chem.* **1990**, *29*, 2883. (b) Poncelet, O.; Hubert-Pfalzgraf, L. G. *Polyhedron* **1990**, *9*, 1305.
- (7) (a) Garbaskas, M. F.; Arendt, R. H.; Kasper, J. S. *Inorg. Chem.* **1987**, *26*, 3191. (b) Hazen, R. M. *The Breakthrough—The Race for the Superconductor*; Summit Book: New York, 1988.
- (8) (a) Benelli, C.; Caneschi, A.; Gatteschi, D.; Guillou, O.; Pardi, L. *Inorg. Chem.* **1990**, *29*, 1750. (b) Goodgame, D. M. L.; Williams, D. J.; Winpenny, R. E. P. *Polyhedron* **1989**, *8*, 1531.
- (9) (a) Evans, W. J.; Sollberger, M. S. *Inorg. Chem.* **1988**, *27*, 4417. (b) Poncelet, O. P.; Sartain, W. J.; Hubert-Pfalzgraf, L. G.; Folting, K.; Caulton, K. G. *Inorg. Chem.* **1989**, *28*, 263.
- (10) Caulton, K. G.; Hubert-Pfalzgraf, L. G. *Chem. Rev.* **1990**, *90*, 969–995.
- (11) Calcd for **2**: $C_{70}H_{24}Y_2Cu_8O_{28} \cdot 4H_2O$: C, 35.69; H, 2.71; N, 10.71. Found: C, 36.47; H, 3.29; N, 10.44.

Synthesis and Structural Characterization of Spontaneously Resolved $[M(aet)_3M'_4O]^{6+}$ ($M = Rh(III), Ir(III)$; $M'_4 = Zn^{II}_4, Co^{II}_4$; aet = 2-Aminoethanethiolate): Conversion of a Linear- to a Cage-Type S-Bridged Polynuclear Structure

There has been considerable research interest in stereochemistry of the S-bridged polynuclear metal complexes with multidentate sulfur-containing ligands such as 2-aminoethanethiolate (aet) and L-cysteinate (L-cys).¹⁻⁷ In particular, *fac(S)*- $[M(aet)_3]$ and

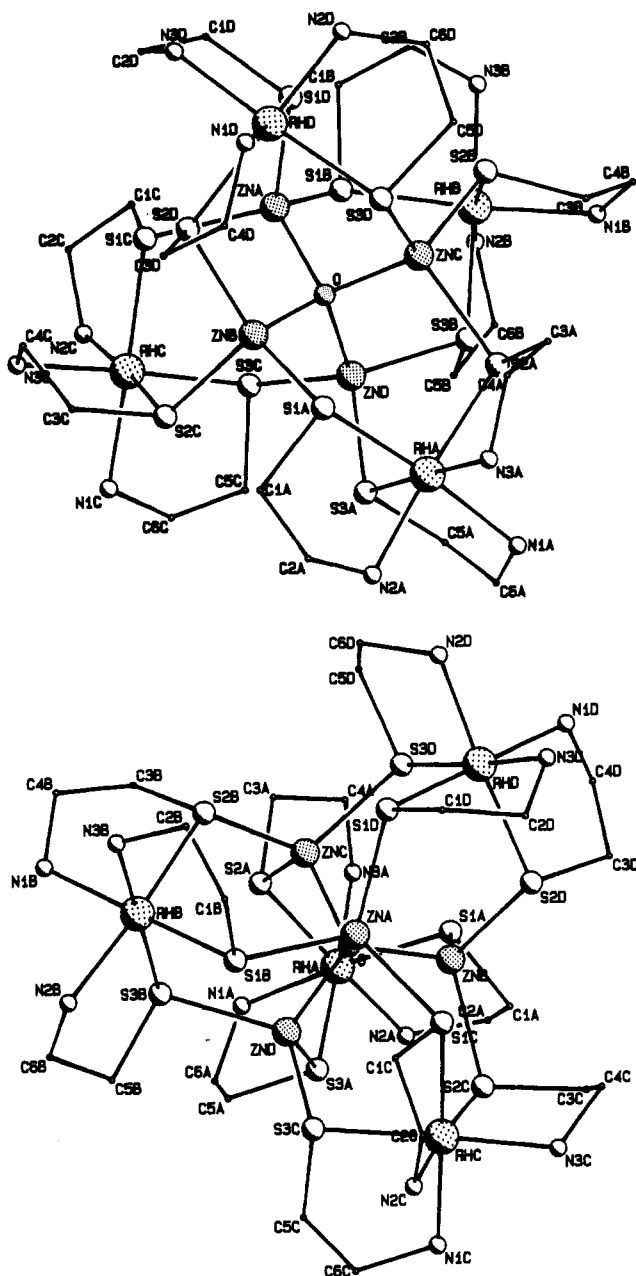


Figure 1. Perspective view of the complex cation of 2 with the atomic labeling scheme: (a, top) view down an axis close to a C_2 axis; (b, bottom) view down an axis close to a C_3 axis.

$fac(S)$ -[M(L-cys-N,S) $_3$] $^{3-}$ (M = Co(III) and Rh(III)) have been recognized to function as S-donating terdentate ligands to a variety

- (1) (a) Bush, D. H.; Jicha, D. C. *Inorg. Chem.* **1962**, *1*, 884. (b) Brubaker, G. R.; Douglas, B. E. *Inorg. Chem.* **1967**, *6*, 1562. (c) DeSimone, R. E.; Ontko, T.; Wardman, L.; Blinn, E. L. *Inorg. Chem.* **1975**, *14*, 1313. (d) Blinn, E. L.; Butler, P.; Chapman, K. M.; Harris, S. *Inorg. Chim. Acta* **1977**, *24*, 139. (e) Heeg, M. J.; Blinn, E. L.; Deutsch, E. *Inorg. Chem.* **1985**, *24*, 1118. (f) Johnson, D. W.; Brewer, T. R. *Inorg. Chim. Acta* **1988**, *154*, 221.
- (2) (a) Konno, T.; Aizawa, S.; Okamoto, K.; Hidaka, J. *Chem. Lett.* **1985**, 1017. (b) Okamoto, K.; Aizawa, S.; Konno, T.; Einaga, H.; Hidaka, J. *Bull. Chem. Soc. Jpn.* **1986**, *59*, 3859. (c) Aizawa, S.; Okamoto, K.; Einaga, H.; Hidaka, J. *Bull. Chem. Soc. Jpn.* **1988**, *61*, 1601. (d) Miyawski, S.; Konno, T.; Okamoto, K.; Hidaka, J. *Bull. Chem. Soc. Jpn.* **1988**, *61*, 2987. (e) Konno, T.; Aizawa, S.; Hidaka, J. *Bull. Chem. Soc. Jpn.* **1989**, *62*, 585. (f) Konno, T.; Aizawa, S.; Okamoto, K.; Hidaka, J. *Bull. Chem. Soc. Jpn.* **1990**, *63*, 792.
- (3) (a) Jicha, D. C.; Busch, D. H. *Inorg. Chem.* **1962**, *1*, 872. (b) Jicha, D. C.; Busch, D. H. *Inorg. Chem.* **1962**, *1*, 878. (c) Wei, C. H.; Dahl, L. F. *Inorg. Chem.* **1970**, *9*, 1878.
- (4) Murase, I.; Ueno, S.; Kida, S. *Bull. Chem. Soc. Jpn.* **1983**, *56*, 2748.

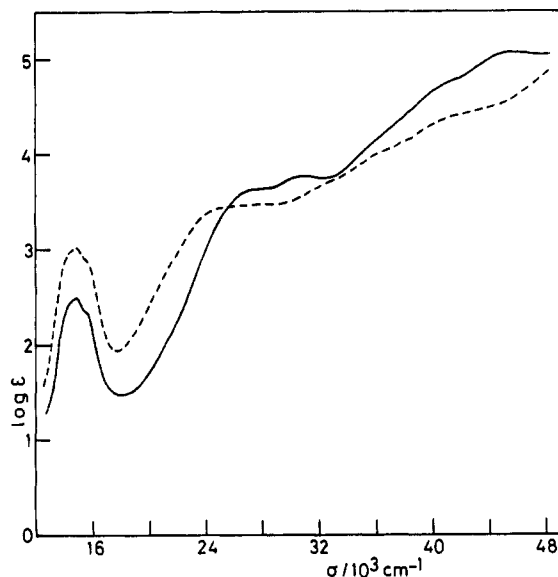


Figure 2. Visible-UV spectra of 2 (—) and 3 (---) in H_2O . ϵ values are given in units of $mol^{-1} dm^3 cm^{-1}$.

of metal ions ($M' = Fe(III)$, $Co(III)$, $Ni(II)$, and $Rh(III)$), forming linear-type S-bridged trinuclear complexes, $[M'\{M(aet$ or $L-cys-N,S)_3\}_2]^{n+}$ or $n-1,2$. From the same point of view, it has been proposed that $fac(S)$ -[M(aet) $_3$] functions as a terdentate ligand to Zn(II) and Cd(II), which prefer to take a tetrahedral geometry, forming linear-type S-bridged polynuclear structures.^{1b,d} However, we have recently found that the reaction of $fac(S)$ -[Rh(aet) $_3$] with $ZnBr_2$ in water does not give a linear-type S-bridged trinuclear complex, but a novel cage-type polynuclear complex, $[[Rh(aet)_3]_4Zn_3O]Br_4$ (1), where each Zn(II) is tetrahedrally coordinated by three sulfur atoms from three different $fac(S)$ -[Rh(aet) $_3$] subunits and a central oxygen atom.⁷ The orange-yellow complex 1, which has a "defective" core $[Zn_3O]^{4+}$,⁸ was spontaneously resolved and showed a drastic CD (circular dichroism) spectral change due to the cleavage of Zn-S bonds in water.⁷ The structure and properties of 1 prompted us to synthesize a cage-type polynuclear complex having a "complete" core $[Zn_4O]^{6+}$ in order to elucidate the structural consequences of metal ions incorporated into the S-bridged polynuclear framework. In this communication, we report the conversion of the linear-type S-bridged trinuclear complexes $[Co^{III}\{M(aet)_3\}_2]^{3+}$ ($M = Rh(III)$, $Ir(III)$)^{2f} to the cage-type octanuclear complexes $[[M(aet)_3]_4M'_4O]^{6+}$ ($M'_4 = Zn^{II}_{4-x}Co^{II}_x$) (2), which have been shown by X-ray diffraction to possess a "complete" core $[M'_4O]^{6+}$.

Treatment of a dark brown aqueous solution containing the linear-type trinuclear complex $[Co^{III}\{Rh(aet)_3\}_2](NO_3)_3 \cdot 3.5H_2O$ (0.5 g)^{2f} with Zn powder (1.5 g) at room temperature produced $[Co^{III}\{Rh(aet)_3\}_2](NO_3)_2$ ^{2f} as a red precipitate in a few minutes, which gradually dissolved to give a pale reddish brown solution. The addition of $ZnBr_2$ (1.5 g) immediately changed the solution color to green. After unreacted Zn powder was filtered off, the green filtrate was allowed to stand at room temperature for 1 day, which gave spontaneously resolved green crystals (2) in 61% yield (0.35 g).⁹ It is noted that the chloride and nitrate salts of this

- (5) (a) Dorfman, J. R.; Rao, Ch. P.; Holm, R. H. *Inorg. Chem.* **1985**, *24*, 453. (b) Rao, Ch. P.; Dorfman, J. R.; Holm, R. H. *Inorg. Chem.* **1986**, *25*, 428. (c) Tremel, W.; Kriege, M.; Krebs, B.; Henkel, G. *Inorg. Chem.* **1988**, *27*, 3886. (d) Rambo, J. R.; Huffman, J. C.; Christou, G. *J. Am. Chem. Soc.* **1989**, *111*, 8027.
- (6) Blower, P. J.; Dilworth, J. R. *Coord. Chem. Rev.* **1987**, *76*, 121.
- (7) Konno, T.; Okamoto, K.; Hidaka, J. *Chem. Lett.* **1990**, 1043.
- (8) Each of four Zn atoms in 1 gave a site occupancy factor of ca. 0.75, which resulted in the formation of the tetravalent complex cation.⁷
- (9) Each crystal that was picked out from the bulk showed a positive or negative CD value at 350 nm. Anal. Calcd for $[[Rh(aet)_3]_4Zn_3.7Co_0.3O]Br_6 \cdot 8H_2O \cdot C_{24}H_{72}N_{12}OS_{12}Co_0.3Zn_3.7Br_6Rh_4 \cdot 8H_2O$: C, 12.96; H, 3.99; N, 7.56; Co, 0.79; Zn, 10.88; Rh, 18.50. Found: C, 12.79; H, 4.20; N, 7.44; Co, 0.76; Zn, 10.42; Rh, 17.78.

complex, which were prepared by using ZnCl_2 or $\text{Zn}(\text{NO}_3)_2$ instead of ZnBr_2 , were also spontaneously resolved. The same reaction of $[\text{Co}^{\text{III}}\{\text{Ir}(\text{aet})_3\}_2](\text{NO}_3)_3 \cdot 3\text{H}_2\text{O}^{10}$ with Zn powder in water, followed by the addition of ZnBr_2 , gave spontaneously resolved deep green crystals (**3**) in 42% yield.¹¹

X-ray structural analysis of the green complex **2** revealed the presence of a discrete hexavalent complex cation and six bromide anions.¹² As shown in Figure 1, the complex cation consists of four octahedral *fac*(S)-[Rh(aet)₃] subunits, four zinc atoms, and one central μ_4 -oxygen atom. The four *fac*(S)-[Rh(aet)₃] subunits are bound in the "complete" tetrahedral core $[\text{Zn}_4\text{O}]^{6+}$ in a tetrahedral arrangement, forming the cage-type S-bridged octanuclear structure. The overall structure of the complex cation of **2** is similar to that of the tetravalent complex cation of **1** with the "defective" core $[\text{Zn}_3\text{O}]^{4+}$.⁷ In particular, the bond angles around the zinc and oxygen atoms in the complex cations of **1** and **2** are quite similar to each other (average S–Zn–S = 111.0 (2)°, S–Zn–O = 108.0 (4)°, and Zn–O–Zn = 109.5 (5)° for **2**; S–Zn–S = 111.8 (2)°, S–Zn–O = 107.1 (4)°, and Zn–O–Zn = 109.5 (5)° for **1**). However, the Rh–S (average 2.344 (5) Å) and Zn–S (average 2.353 (5) Å) bond lengths in **2** are somewhat longer than the corresponding bond lengths in **1** (average Rh–S = 2.322 (6) Å and Zn–S = 2.338 (6) Å), and the Zn–O bond lengths (average 1.97 (1) Å) are somewhat shorter than the Zn–O ones observed in **2** (1.99 (1) Å), reflecting the structural difference between the $[\text{Zn}_4\text{O}]^{6+}$ core and the $[\text{Zn}_3\text{O}]^{4+}$ one.

The complex cation of **2** has two kinds of chiral configurations, Δ or Λ for the *fac*(S)-[Rh(aet)₃] subunits and *R* or *S* for the bridging sulfur atoms. For the spontaneously resolved (–)^{CD}₃₅₀-[[Ir(aet)₃]₄Zn₄O]⁶⁺ cation, it was determined by the anomalous scattering technique¹³ that all four *fac*(S)-[Rh(aet)₃] subunits take Δ and all 12 bridging sulfur atoms take *S*, as shown in Figure 1. This assignment is consistent with the fact that the reaction of $\Delta\Delta\text{-}[\text{Co}\{\text{Rh}(\text{aet})_3\}_2]^{3+}$ with Zn powder gave the (–)^{CD}₃₅₀ isomer.

In contrast to the orange-yellow complex **1** with the "defective" core $[\text{Zn}_3\text{O}]^{4+}$, the green complex **2** shows no significant absorption and CD spectral change in water for several hours, indicating that the cage-type S-bridged octanuclear structure with the "complete" core is fairly stable in solution. The visible–UV absorption spectrum of **2**¹⁴ is similar to that of **1**⁷ in the energy region higher

than $20 \times 10^3 \text{ cm}^{-1}$, showing the two spin-allowed d–d absorption bands (27.9 and $31.03 \times 10^3 \text{ cm}^{-1}$) and the sulfur-to-rhodium charge-transfer band ($45.66 \times 10^3 \text{ cm}^{-1}$). In the corresponding region, the CD spectral pattern of **2** is also similar to that of **1**, showing a major negative CD band ($26.67 \times 10^3 \text{ cm}^{-1}$) in the d–d absorption band region and negative ($42.74 \times 10^3 \text{ cm}^{-1}$) and positive ($46.95 \times 10^3 \text{ cm}^{-1}$) CD bands in the charge-transfer band region for the $\Delta\Delta\Delta\Delta$ isomer. However, **2** exhibits an additional absorption band composed of three components at $14.53 \times 10^3 \text{ cm}^{-1}$, as illustrated in Figure 2. A quite similar absorption band has been recognized for the tetrahedral Co(II) complexes having the $\text{Co}^{\text{II}}\text{S}_4$ chromophore,^{5a,15} which has been assigned as a spin-allowed d–d transition (${}^4\text{A}_2(\text{F}) \rightarrow {}^4\text{T}_1(\text{P})$). The plasma emission spectral analysis of **2** pointed out the presence of cobalt atom in a ratio Rh:Zn:Co = 4:3.7:0.3 ratio.⁹ These facts suggest that a slight amount of Co(II) is trapped in place of Zn(II) in $[\{\text{Rh}(\text{aet})_3\}_4\text{Zn}_4\text{O}]^{6+}$.

In the analogous deep green Ir(III) cage-type complex (**3**), Co(II) is trapped in a much higher ratio (Ir:Zn:Co = 4:2.8:1.2).¹¹ Consistent with this result, the additional absorption band (ca. $14.5 \times 10^3 \text{ cm}^{-1}$) of **3**¹⁶ is intensified in comparison with that of **2** (Figure 2). X-ray structural analysis¹⁷ indicated that the complex cation of **3**, $([\{\text{Ir}(\text{aet})_3\}_4\text{M}'_4\text{O}]^{6+})$ ($\text{M}'_4 = \text{Zn}_{2.8}\text{Co}_{1.2}$), is almost isostructural with the complex cation of **2**, and the bond lengths and angles in **3** are very similar to those in **2**. However, it is noted that the Ir–S bond lengths in **3** (average 2.336 (7) Å) are somewhat shorter than the Rh–S ones in **2** (average 2.344 (5) Å).

For the spontaneously resolved (–)^{CD}₃₀₀-[[Ir(aet)₃]₄M'₄O]⁶⁺, the chiral configurations are regulated to Δ for the four *fac*(S)-[Ir(aet)₃] subunits and *S* for the 12 bridging sulfur atoms, as in the case of **2**.¹⁸ Molecular model constructions reveal that a significant nonbonding interaction comes into exist among the aet chelate rings of adjacent *fac*(S)-[M(aet)₃] subunits when the absolute configuration of the four subunits is not uniform. Furthermore, each of the ¹³C NMR spectra of **2** and **3** showed two signals due to two kinds of methylene carbon atoms of the aet ligand,¹⁹ suggesting that only the $\Delta\Delta\Delta\Delta$ and $\Lambda\Lambda\Lambda\Lambda$ isomers with a T symmetry are formed for $[\{\text{M}(\text{aet})_3\}_4\text{M}'_4\text{O}]^{6+}$. Accordingly, either the Δ or the Λ isomer of *fac*(S)-[M(aet)₃] is selectively incorporated in the cage-type $[\{\text{M}(\text{aet})_3\}_4\text{M}'_4\text{O}]^{6+}$ structure, and the spontaneous resolution observed in the present

- (10) $[\text{Co}^{\text{III}}\{\text{Ir}(\text{aet})_3\}_2]^{3+}$ was prepared from *fac*(S)-[Ir(aet)₃], Co^{2+} , and H_2O_2 by a method similar to that used for $[\text{Co}^{\text{III}}\{\text{Rh}(\text{aet})_3\}_2]^{3+}$. Anal. Calcd for $[\text{Co}\{\text{Ir}(\text{aet})_3\}_2](\text{NO}_3)_3 \cdot \text{H}_2\text{O}$, $\text{C}_{12}\text{H}_{36}\text{N}_9\text{O}_9\text{S}_6\text{CoIr}_2$: C, 13.05; H, 3.46; N, 11.42; Co, 5.34. Found: C, 13.24; H, 3.49; N, 11.41; Co, 5.10.
- (11) Each crystal that was picked out from the bulk showed a positive or negative CD value at 300 nm. Anal. Calcd for $[\{\text{Ir}(\text{aet})_3\}_4\text{Zn}_4\text{O}]^{6+} \cdot 9.5\text{H}_2\text{O}$: C, 11.07; H, 3.52; N, 6.46; Co, 2.72; Zn, 7.03; Ir, 29.54. Found: C, 11.19; H, 3.44; N, 6.53; Co, 2.65; Zn, 6.86; Ir, 28.86.
- (12) Crystal data for $[\{\text{Rh}(\text{C}_2\text{H}_5\text{NS})_3\}_4\text{Zn}_4\text{O}] \cdot 8\text{H}_2\text{O}$ at 293 K: $M_r = 2226.4$, $0.25 \times 0.17 \times 0.10$ mm, orthorhombic, $P2_12_12_1$, $a = 18.924$ (3) Å, $b = 18.925$ (3) Å, $c = 18.919$ (3) Å, $V = 6775$ (2) Å³, $Z = 4$, $D_{\text{calc}} = 2.18 \text{ g cm}^{-3}$, $\lambda(\text{Mo K}\alpha) = 0.71069$ Å, $\mu(\text{Mo K}\alpha) = 60.79 \text{ cm}^{-1}$, R (R_w) = 0.0599 (0.0536) for 4649 independent reflections with $F_o > 3\sigma(F_o)$ ($2\theta < 50^\circ$). The structure was solved by direct methods (MULTAN-80) and difference Fourier techniques and refined by full-matrix least-squares methods using anisotropic thermal parameters for non-hydrogen atoms. All calculations were performed with use of the programs of SHELX-76. Each atom of the mixed Zn/Co site (0.925 Zn; 0.075 Co) was refined as a Zn atom with a site occupancy factor of 1.0. One of the six independent bromide anions exhibited positional disorder, which appeared to be distributed in three different locations (Br(6A), Br(6B), and Br(6C)) with a site occupancy factor of 1/3. Three of nine H₂O oxygen atoms (O(7W), O(8W), and O(9W)) were refined with a site occupancy factor of 2/3. Selected bond lengths (Å) and angles (deg) (averaged): Rh–S, 2.344 (5); Rh–N, 2.12 (2); Zn–S, 2.353 (5); Zn–O, 1.97 (1); S–Rh–S, 95.1 (2); N–Rh–N, 91.3 (6); Zn–S–Rh, 112.8 (2); S–Zn–S, 111.0 (2); O–Zn–S, 108.0 (4); Zn–O–Zn, 109.5 (5).
- (13) The crystal used for the X-ray structural analysis showed a negative CD value at 350 nm. For atomic parameters containing the Δ configuration of *fac*(S)-[Rh(aet)₃] subunits, $R = 0.0599$ and $R_w = 0.0536$ ($w = 1.3204/(\sigma^2(F_o) + 0.000862(F_o)^2)$), and for that containing the Λ configuration, $R = 0.0694$ and $R_w = 0.0648$ ($w = 1.4638/(\sigma^2(F_o) + 0.001065(F_o)^2)$). Thus, the (–)^{CD}₃₅₀ isomer is assigned to take the $\Delta\Delta\Delta\Delta$ configuration. The enantiomeric structure could be rejected at the 0.005 significance level by the Hamilton test: Hamilton, W. C. *Acta Crystallogr.* **1965**, *18*, 502.

- (14) Visible–UV spectrum of **2**, H₂O solvent [λ_{max} , 10^3 cm^{-1} (log ϵ ; ϵ in mol^{–1} dm³ cm^{–1}): 14.5 (2.45 sh), 14.86 (2.48), 15.5 (2.33 sh), 27.9 (3.40 sh), 31.01 (3.53), 41.7 (4.51 sh), 45.66 (4.81). The sh label denotes a shoulder.
- (15) (a) Lane, R. W.; Ibers, J. A.; Frankel, R. B.; Papaefthymiou, G. C.; Holm, R. H. *J. Am. Chem. Soc.* **1977**, *99*, 84. (b) Nakata, M.; Ueyama, N.; Nakamura, A.; Nozawa, T.; Hatano, M. *Inorg. Chem.* **1983**, *22*, 3028.
- (16) Visible–UV spectrum of **3**, H₂O solvent [λ_{max} , 10^3 cm^{-1} (log ϵ ; ϵ in mol^{–1} dm³ cm^{–1}): 14.6 (2.98 sh), 14.84 (3.00), 15.5 (2.88 sh), 27.93 (3.45), 37.0 (4.02 sh), 43.1 (4.41 sh), 50.25 (4.93). The sh label denotes a shoulder.
- (17) Crystal data for $[\{\text{Ir}(\text{C}_2\text{H}_5\text{NS})_3\}_4\text{Zn}_{2.8}\text{Co}_{1.2}\text{O}] \cdot 9.5\text{H}_2\text{O}$ at 293 K: $M_r = 2603.0$, $0.17 \times 0.15 \times 0.15$ mm, orthorhombic, $P2_12_12_1$, $a = 19.092$ (2) Å, $b = 19.097$ (2) Å, $c = 19.099$ (2) Å, $V = 6963$ (1) Å³, $Z = 4$, $D_{\text{calc}} = 2.48 \text{ g cm}^{-3}$, $\lambda(\text{Mo K}\alpha) = 0.71069$ Å, $\mu(\text{Mo K}\alpha) = 123.67 \text{ cm}^{-1}$, R (R_w) = 0.0634 (0.0634) for 5267 independent reflections with $F_o > 3\sigma(F_o)$ ($2\theta < 50^\circ$). Each atom of the mixed Zn/Co site (0.7 Zn; 0.3 Co) was refined as a Zn atom with a site occupancy factor of 0.97. Four of the six independent bromide anions exhibited positional disorder and were best modeled with two positions for each atom. Two of ten H₂O oxygen atoms (O(9W) and O(10W)) were refined with a site occupancy factor of 0.75. Selected bond lengths (Å) and angles (deg) (averaged): Ir–S, 2.335 (7); Ir–N, 2.12 (3); Zn(Co)–S, 2.344 (8); Zn(Co)–O, 1.96 (2); S–Ir–S, 95.7 (3); N–Ir–N, 91.4 (10); Zn(Co)–S–Rh, 112.6 (3); S–Zn(Co)–S, 110.6 (3); O–Zn(Co)–S, 108.3 (6); Zn(Co)–O–Zn(Co), 109.5 (8).
- (18) The crystal used for the X-ray structural analysis showed a negative CD value at 300 nm. For atomic parameters containing the Δ configuration of *fac*(S)-[Ir(aet)₃] subunits, $R = 0.0634$ and $R_w = 0.0634$ ($w = 1.1095/(\sigma^2(F_o) + 0.003073(F_o)^2)$), and for that containing the Λ configuration, $R = 0.0768$ and $R_w = 0.0784$ ($w = 1.3941/(\sigma^2(F_o) + 0.002867(F_o)^2)$). Thus, the (–)^{CD}₃₀₀ isomer is assigned to take the $\Delta\Delta\Delta\Delta$ configuration.
- (19) ¹³C NMR in D₂O (ppm from DSS): 33.64 (–CH₂S) and 51.20 (–C–H₂NH₂) for **2**; 33.32 (–CH₂S) and 52.65 (–CH₂NH₂) for **3**.

work may be related to this high symmetrical structure.

Supplementary Material Available: Tables A-F, listing atomic coordinates and equivalent isotropic thermal parameters, bond distances and angles, and anisotropic thermal parameters for 2 and 3 (14 pages). Tables G and H, listing observed and calculated structure factors for 2 and 3, respectively (42 pages). Ordering information is given on any current masthead page.

Department of Chemistry
University of Tsukuba
Tsukuba, Ibaraki 305, Japan

Takumi Konno*
Ken-ichi Okamoto
Jinsai Hidaka

Received January 3, 1991

$(\text{Et}_3\text{P})_6\text{Co}_6\text{Te}_8$ and a Connection between Chevrel Clusters and the NiAs Structure

We have shown several examples¹ of molecule-to-solid transformations in which we have been able to intercept and characterize reaction intermediates. In some of these cases,^{1a,b} we have isolated molecule intermediates that bear no particular resemblance to the ultimate solid products; however, in other instances^{1c-e}, we have found cluster intermediates that are identifiable fragments of the solid lattice. In this communication we report a molecular precursor synthesis of β -cobalt telluride and the interception of the intermediate $(\text{Et}_3\text{P})_6\text{Co}_6\text{Te}_8$ (1). We show that this core is, furthermore, a simply distorted fragment of the CoTe (NiAs-type) lattice.

Since dicobalt octacarbonyl² and triethylphosphine telluride³ are convenient sources of Co(0) and Te(0), respectively, we attempted to find the conditions under which the combination of the two would yield cobalt telluride. We found⁴ that the reaction of $\text{Co}_2(\text{CO})_8$ with $\text{Et}_3\text{P}\text{Te}$ in a 3:8 molar ratio gave cluster 1. The compound is a very dark red, crystalline solid that is soluble in common organic solvents. We determined the molecular structure of the compound,⁵ and a drawing of that structure is shown in

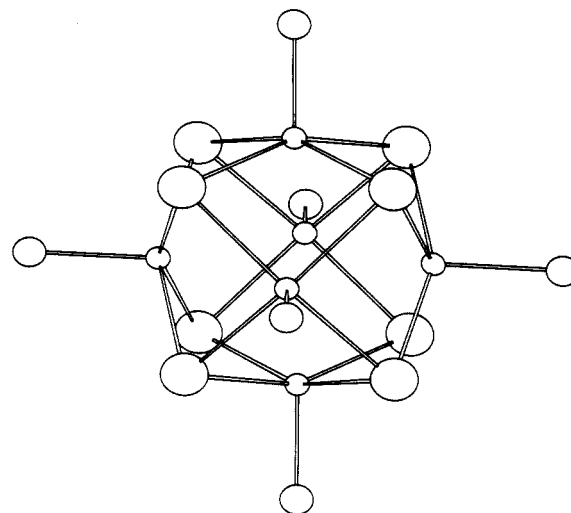


Figure 1. Molecular structure of $\text{Co}_6\text{Te}_8(\text{PEt}_3)_6$. Small circles represent Co atoms. Large circles represent Te atoms. Intermediate circles represent P atoms. C_2H_5 groups are omitted for clarity. Selected averages: $r(\text{Co}-\text{Te}) = 2.521$ (4) Å (average of 34, std dev = 0.008 Å); $r(\text{Te}-\text{Te}) = 3.483$ (3) Å (average of 19, std dev = 0.014 Å); $r(\text{Co}-\text{P}) = 2.139$ (9) Å (average of 6, std dev = 0.010 Å); $\theta(\text{Co}-\text{Te}-\text{Co}) = 79.53$ (13)° (average of 24, std dev = 0.46°); $\theta_{\text{cis}}(\text{Te}-\text{Co}-\text{Te}) = 87.38$ (13)°, std dev = 0.58°; $\theta_{\text{trans}}(\text{Te}-\text{Co}-\text{Te}) = 155.29$ ° (average of 12, std dev = 0.53°); $\theta(\text{Te}-\text{Co}-\text{P}) = 102.3$ (3)° (average of 24, std dev = 1.8°). There are two independent clusters in the unit cell. The structures of the two are essentially identical.

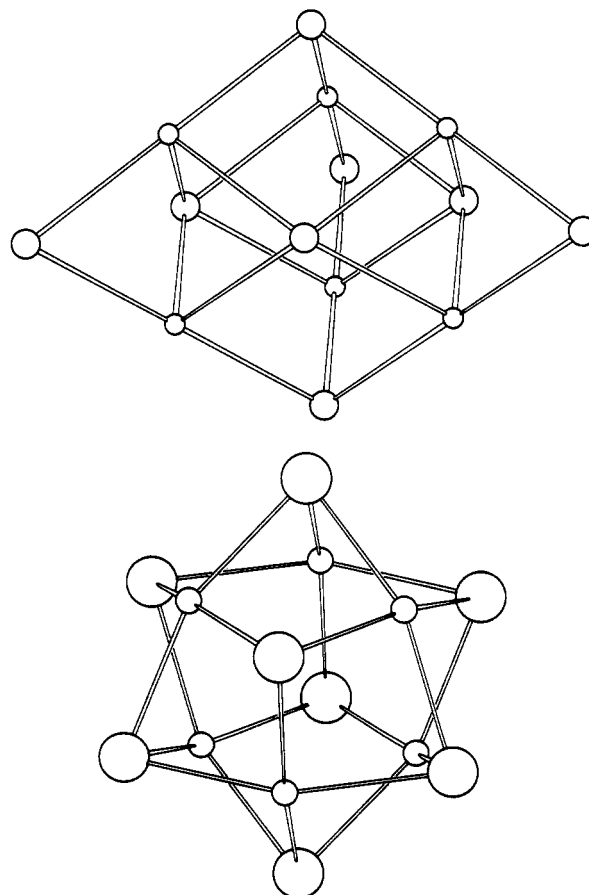


Figure 2. (a) Top: Void site in the CoTe lattice. Large circles represent Te; small circles represent Co. (b) Bottom: Co_6Te_8 core of 1 redrawn to stress relationship with the void site shown in part a.

Figure 1. The structure is composed of an octahedron of Co atoms with a Te atom on each octahedral face. The surface of the cluster is passivated by a triethylphosphine ligand bound to each cobalt. This cluster is a member of the growing family of Chevrel-type⁶

- (1) (a) Steigerwald, M. L.; Rice, C. E. *J. Am. Chem. Soc.* **1988**, *110*, 4228. (b) Steigerwald, M. L. *Chem. Mater.* **1989**, *1*, 52. (c) Brennan, J. G.; Siegrist, T.; Carroll, P. J.; Stuczynski, S. M.; Brus, L. E.; Steigerwald, M. L. *J. Am. Chem. Soc.* **1989**, *111*, 4141. (d) Brennan, J. G.; Siegrist, T.; Stuczynski, S. M.; Steigerwald, M. L. *J. Am. Chem. Soc.* **1989**, *111*, 9240. (e) Brennan, J. G.; Siegrist, T.; Stuczynski, S. M.; Steigerwald, M. L. *J. Am. Chem. Soc.* **1990**, *112*, 9233.
- (2) Wender, I.; Pino, P. *Organic Synthesis via Metal Carbonyls*; Wiley-Interscience: New York, 1968; Vol. 1.
- (3) Zingaro, R. A.; Stevens, B. H.; Irgolic, K. *J. Organomet. Chem.* **1965**, *4*, 320-3.
- (4) The synthesis of 1 was as follows. Dicobalt octacarbonyl (2.06 g, 6.0 mmol) was dissolved in toluene (40 mL) and treated with triethylphosphine (4 mL, 27 mmol) and triethylphosphine telluride (4.12 g, 16.8 mmol). The resulting mixture was heated to reflux for 2 h, then cooled to room temperature, and filtered. The toluene solution was concentrated in vacuo, and pentane was added. Crystallization at -20 °C gave 2.60 g of a dark, crystalline solid. Residual CO (shown by infrared spectroscopy) was exchanged as follows: A portion of the crude product (1.89 g) was dissolved in toluene (30 mL) and treated with triethylphosphine (2.8 mL, 19 mmol). The mixture was heated to reflux 17 hr. Crystallization as above gave 1 (1.65 g, 55% effective overall yield) as a black-red crystalline solid. The infrared spectrum of this solid showed no CO. The compound was characterized as follows IR (CS_2): in addition to the trace CO band (1930 cm^{-1}), there are only absorptions characteristic of coordinated Et_3P . $^1\text{P}\{^1\text{H}\}$ NMR (C_6D_6): 88.1 ppm downfield from (external) 85% H_3PO_4 ; fwhm = 710 Hz. UV-vis (toluene), λ_{max} (ϵ): 398 (37000), 474 (23700), 538 nm (20000). The compound decomposes without melting. (The thermal behavior of this compound is discussed in the text.) Anal. (Analytische Laboratorien). Found (calcd for $\text{C}_{36}\text{H}_{90}\text{Co}_6\text{P}_6\text{Te}_8$): C, 20.86 (20.75); H, 4.23 (4.35); Co, 17.10 (16.97); P, 8.74 (8.92); Te, 49.00 (49.00).
- (5) Compound 1 crystallizes in the $P\bar{1}$ space group. Lattice constants: $a = 12.2460$ (10) Å, $b = 13.1120$ (10) Å, $c = 20.4420$ (20) Å, $\alpha = 88.790$ (10)°, $\beta = 86.480$ (10)°, $\gamma = 70.780$ (10)°, $Z = 2$, $V = 3093.6$ (5) Å³. There are two independent clusters in the unit cell. Data collection and reduction: $2\theta_{\text{max}} = 44.8$ °, 5729 reflections with $I > 2.5\sigma$. The last least-squares cycle was calculated with 56 atoms, 326 parameters, and 5729 out of 7999 reflections; $R = 0.069$, $R_w = 0.058$.